
PREDICTING CHEMICALLY ACCURATE ADSORPTION ENERGY USING AN INTERPRETABLE DEEP LEARNING MODEL PRETRAINED BY GGA CALCULATION DATA

Zhihao Zhang¹ and Xiao-Ming Cao^{1,2,*}

¹State Key Laboratory of Green Chemical Engineering and Industrial Catalysis, Centre for Computational Chemistry and Research Institute of Industrial Catalysis, East China University of Science and Technology, Shanghai 200237, P. R. China

²State Key Laboratory of Synergistic Chem-Bio Synthesis, School of Chemistry and Chemical Engineering, Shanghai Jiao Tong University, Shanghai 200240, P. R. China

*Corresponding author: xmcao@sjtu.edu.cn

July 29, 2025

ABSTRACT

Molecular adsorption energy is a critical descriptor for high-throughput screening of heterogeneous catalysts and electrode materials. However, precise experimental adsorption energies are scarce due to the complexity of experiments, while density functional theory (DFT) calculations remain computationally expensive for large-scale material screening. Machine learning models trained on DFT data have emerged as a promising alternative, but face challenges such as functional dependency, limited labeled high-fidelity data, and interpretability issues. Herein, we present DOS Transformer for Adsorption (DOTA), a novel deep learning model that leverages local density of states (LDOS) as input to predict chemically accurate adsorption energies across metallic and intermetallic surfaces. DOTA integrates multi-head self-attention mechanisms with LDOS feature engineering to capture orbital interaction patterns, achieving superior accuracy and transferability. Pretrained on PBE-level DFT data, DOTA can be fine-tuned using minimal high-fidelity experimental or hybrid functional data to predict adsorption energies with chemical accuracy. The model resolves long-standing challenges, such as the "CO puzzle" and outperforms traditional theories, like the d-band center and Fermi softness models. It provides a robust framework for efficient catalyst and electrode screening, bridging the gap between computational and experimental approaches.

Introduction

Molecular adsorption energy has been widely used as a descriptor for high-throughput screening of heterogeneous catalysts and electrode materials. [1, 2, 3, 4, 5, 6, 7, 8] Due to the substantial inherent uncertainties arising from the facts, such as side reactions, surface defects, and impurities in most experiments, precise experimental adsorption energies could only be obtained through single-crystal adsorption microcalorimetry with an elaborate experimental design so far, resulting in scarce benchmark experimental data. [9, 10, 11, 12, 13, 14, 15, 16, 17] This limits the application in screening candidate materials. Consequently, the adsorption energies derived from density functional theory (DFT) calculations have been extensively applied for materials screening. [18, 19, 20, 21, 22] Yet, it is not easy to afford the huge computational cost of DFT calculations to achieve a great number of adsorption energies at various active site ensembles in multi-component alloys. Therefore, machine learning models trained using data labeled by DFT calculations have recently emerged as a promising method to predict the adsorption energy for material screening. [23, 24, 25, 26, 27, 28, 29, 30, 31] Furthermore, the deep learning model demonstrated superior generalization and transferability for a broader range of adsorbates and catalysts compared with surrogate models utilizing a small dataset for specific adsorbates and materials. [32, 33, 34, 35, 36] Notably, machine learning interatomic potentials, which obtain

optimized adsorbate structures and adsorption energies using structure coordinates as inputs, have been established as a critical technique in recent years. [37, 38, 39, 40, 41]

However, the prediction of chemically accurate adsorption energies using labeled DFT calculation data remains a significant challenge. For one thing, the reduced symmetry of surface adsorption structures increases the computational cost of DFT calculations to label each data point compared to bulk materials and molecules. For another, the low symmetry necessitates more than two orders of magnitude more surface adsorption data for machine learning model training than bulk materials and molecules. [42] Consequently, this results in significantly scarcer labeled adsorption data compared to molecular and bulk material data, despite the development of several databases such as Open Catalyst and Catalysis-Hub. [43, 44, 45] Furthermore, it is challenging to leverage limited labeled adsorption data for model training. The labeled DFT data frequently originate from different exchange-correlation functionals and calculation parameter settings, such as different basis sets, k-point samplings, and versions of pseudopotentials, indicating inconsistent and discontinuous potential energy surface data for the training of machine learning interatomic potential. As a result, only a small portion of the labeled data with consistent exchange-correlation functional and calculation parameter settings in the databases were utilized in most of the previous work in a single task. [46, 47, 48, 49, 50]

More importantly, the accuracy of the predicted adsorption energy based on the deep learning model is subject to the exchange-correlation functional utilized for the training set, rendering it functional-dependent. The constraint of computational cost renders the adsorption databases to be predominantly composed of the results based on generalized gradient approximation (GGA) exchange-correlation functionals up to now, particularly the PBE [51] functional. [52, 53] However, the PBE functional exhibits limitations in terms of accuracy, exemplified by the classic "CO puzzle" problem. [54, 55, 56, 57, 58] Moreover, the meta-GGA functionals of SCAN [59] and r^2 SCAN [60], which have been regarded as the promising functionals to establish a reliable adsorption database recently, even overbind slightly compared to PBE and mistakenly predict the preferential site for CO adsorption as well. [61] The substantial computational cost associated with high-level quantum chemistry methods, such as random phase approximation (RPA) [62], which can yield chemically accurate adsorption energies using the embedding strategy, [63, 64, 65, 66] precludes their use in constructing a sufficiently large dataset for model training. The Δ -machine learning method presents an alternative approach for predicting chemically accurate adsorption energies for specific systems by incorporating RPA calculation results. Nevertheless, approximately one hundred RPA results are still required to train a model to predict CO adsorption energies on a specific metal surface using the Δ -machine learning method. [67, 68, 69, 70] Consequently, the extension of the method to vast chemical compound spaces is hindered by significant computational expenditures. Thus, the application of this method to catalyst and electrode screening is severely limited due to these constraints. It is imperative to develop a new model and protocol to predict chemically accurate adsorption energies, making full use of the limited GGA-level data available.

To this end, breaking the limitation of functional-dependency is a prerequisite for a new machine learning model for precise adsorption prediction. As illustrated in **Fig. 1a**, the machine learning interatomic potential, which corresponds to the mapping from input atomic coordinates to output energies, must be functional-dependent, arising from the intrinsic functional-independency of atomic coordinates, while the functional-dependency of energies. This indicates that a functional-independent deep learning model may be achieved by employing functional-dependent physical quantities as both model input and output. Notably, both adsorption energies and electronic structure characteristics exhibit strong functional-dependency. The density of states (DOS) serves as an information-dense descriptor that compresses a substantial amount of spatially distributed electronic structure information into a computationally affordable one-dimensional energy space, making it a promising candidate as a model input to overcome the limitation of functional-dependency.

Interestingly, DOS is one of the most frequently used physical quantities that help to understand the chemisorption strength in heterogeneous catalysis. In particular, the d-band center theory, [71, 72], which is derived from the approximation of the Newns-Anderson model, [73, 74, 75] is prevalent in the field of heterogeneous catalysis. Recently, Xin's group proposed a Bayesian learning method to emphasize the significance of the orbital orthogonalization term in the Newns-Anderson model for noble metal surfaces, which was previously omitted in the d-band center theory. [76] Fermi softness offers an alternative explanation for the orbital contribution to adsorption by extending the frontier molecular orbital theory to the solid surface. [77] This approach underscores the critical role of the DOS near the Fermi levels. Fung et al. proposed a deep convolutional neural network (DOSNet) to predict the adsorption energy at the GGA level by utilizing the local density of states (LDOS) of the adsorbate and the binding sites of the substrate, mainly based on the adsorbed structures. [78] Nevertheless, the CNN featurizer in DOSNet suffers from low explainability and long-range interaction neglect [79, 80, 81, 82, 83], which limits the comprehensive understanding of the contribution of different energy levels to the adsorption.

Despite extensive studies on the relationship between adsorption energies and DOS, the fundamental challenge of functional-dependency for adsorption strength remains unaddressed. Herein, we present a new deep learning model,

called DOS Transformer for Adsorption (DOTA), to efficiently predict accurate adsorption energies across metallic and intermetallic surfaces. The DOTA architecture synergistically integrates the interpretable multi-head self-attention mechanism of the Transformers framework with LDOS feature engineering to first capture the underlying modes of orbital interactions through pretraining using PBE-level LDOS profiles and adsorption energies without prior physical constraints. The functional-independent orbital interaction modes enable transfer learning across quantum chemistry methods and experimental data. Therefore, the chemically accurate adsorption energies of a specific adsorbate across various metallic and intermetallic surfaces could be predicted by fine-tuning the PBE-level model through incorporating the LDOS profile of the gaseous adsorbate at the HSE06 [84] level and few-shot precise experimental adsorption energies. We also comprehensively revisited the d-band center theory and Fermi softness through our interpretable attention paradigm and deciphered the CO/Pt(111) puzzle.

Results

Workflow of DOTA

The DOTA framework employs a two-stage training protocol comprising pretraining and fine-tuning steps to predict chemically precise adsorption energies, as schematically illustrated in **Fig. 1b**. During the pretraining step, all LDOS inputs and corresponding chemisorption energy outputs were derived from PBE results, thereby constructing a DOTA-PBE model. This model establishes fundamental orbital interaction patterns between adsorbates and metallic surfaces and predicts precise PBE adsorption energies of the trained adsorbates across metallic and intermetallic surfaces. Subsequent fine-tuning integrated GGA-level LDOS-adsorption energy pairs and hybrid data consisting of the HSE06-level DOS profile of the gaseous molecule and few-shot experimental adsorption energies of the studied adsorbate to achieve accurate adsorption energies of the studied adsorbate. To enable efficient catalyst screening without requiring preliminary time-consuming geometry optimization, DOTA strategically processes gaseous adsorbate LDOS and bare surface LDOS instead of adsorbed complex configurations. The model architecture implements quantum mechanically informed feature engineering, allocating 32 angular momentum-projected density of states (PDOS) embedding channels per surface atom and 8 PDOS embedding channels per adsorbate atom. For instance, the bridge-site adsorption configuration corresponds to 64 surface atom channels (2 atoms \times 32 channels) and 8 adsorbate atom channels. This channel design ensures compatibility with f-electron systems and spin-polarized calculations. Initial feature processing involved an average pooling layer to normalize energy interval disparities across different DOS calculations. Surface and adsorbate channels were then projected into separate latent spaces through weight-shared fully connected layers with nonlinear activation functions. The multi-head attention mechanism in Transformer architecture enables efficient modelling of long-range orbital interactions across the entire energy spectrum, capturing the interactions between orbitals with different angular momentum quantum numbers. Final energy predictions are generated by merging surface atom features through flattening and sequential fully connected layer processing. Comprehensive implementation details regarding network architecture and hyperparameter selection are provided in the Methods section.

Performance of DOTA-PBE

The pretraining dataset was constructed using 23,861 PBE chemisorption energies involving 11 different adsorbates. These encompassed monoatomic adsorbates (H, C, N, O, and S) and their hydrogenated counterparts (CH, CH₂, CH₃, NH, OH, H₂O, and SH) across 1,982 distinct metallic and intermetallic (111) surfaces comprising 37 metallic elements. The selected adsorbates cover molecules with varying degrees of bonding unsaturation, rendering the chemisorption energies to span from near 0 eV to over -10 eV. This broad energy range provides comprehensive sampling of the diversity of adsorption strengths, ensuring adequate coverage of chemical environments relevant to catalytic processes.

Fig. 2a illustrates the predictive performance of the PBE-level DOTA model via 5-fold cross-validation on the pre-training PBE dataset. The Transformer-based architecture achieves exceptional accuracy of the DOTA-PBE model with a mean absolute error (MAE) of 0.066 eV and a mean absolute percentage error (MAPE) of 1.53% across all the adsorption systems. Adsorbate-specific analysis reveals MAE ranging from 0.042 eV for monoatomic H to 0.096 eV for NH. MAE differences among different adsorbates arise from the bonding unsaturation and resulting adsorption strength. The stronger adsorption, the higher MAE, but the lower MAPE. This complementary behavior of error metrics exhibits the necessity of taking both absolute (MAE) and relative (MAPE) error measures into account when assessing model performance, particularly given the wide energy range in the dataset. Notably, the reliance on electronic structure features rather than geometric parameters enables effective transferability between adsorbates with analogous bonding characteristics. We also tested the OH adsorption atop (111) surfaces. The tested surfaces were not included in the previous pretraining PBE dataset. As shown in **Fig. 2b**, the d-band center theory fails at the sites composed of the group 13-14 elements that rely on the s and p orbitals for bonding, while the accuracy of the DOTA-PBE model is element-independent across the metallic and intermetallic surfaces (**Fig. 2c**). Moreover, it indicates that hydrogenated

derivatives may be accurately modelled with minimal additional training data. The electronic structure-based approach of DOTA exhibits robust predictive capability across diverse chemical environments.

We further compared the performance of the DOTA-PBE model with the d-band center and Fermi softness models. We first take the chemisorption of OH over the top site of Ag(111) and Au(111) surfaces as an example, which was not included in our pretraining dataset. As shown in **Fig. 3a**, the d-band of the Ag(111) surface is mainly concentrated in the energy window far below the Fermi level, implying weakened adsorption if following Fermi softness theory. This is not in good agreement with the PBE calculation result of -1.67 eV for the adsorption of OH atop the Ag(111) surface. Moreover, the decomposition of the contribution of each energy level (**Fig. 3b**) by the integrated gradients algorithm suggests that those energy levels far below the Fermi level made the main contribution for OH adsorption atop Ag(111) rather than those energy levels around the Fermi level. Interestingly, the lower d-band center of Ag(111) ($\varepsilon_d = -3.61$ eV) than Au(111) surface ($\varepsilon_d = -3.00$ eV), however, results in the stronger adsorption of OH atop Ag(111) than Au(111) (-1.01 eV). These errors may be attributed to the fact that both the d-band center and the Fermi softness theories are based on the presumption of covalent bonding, while the electron transfer from the metallic surface to the singly occupied molecular orbital of OH [85] or Pauli repulsion [86], rather than the orbital overlapping between OH and the Ag(111) or Au(111) surface, dominates the chemisorption of OH atop Ag(111) or Au(111). In contrast, our DOTA-PBE model, which omits any predefined restriction, can accurately predict the adsorption energies of OH atop Ag(111) and Au(111) surfaces, with a prediction of -1.71 eV and -1.13 eV, respectively.

The H adsorption over Pt₃Y(111) is a classic example that d-band center theory fails to predict the adsorption site.[77] PBE calculations show that the adsorption energy of H atop the Pt site is -2.80 eV, while it is -0.81 eV atop the Y site, indicating that H tends to preferentially adsorb at the Pt site. However, the Pt site has a lower d-band center ($\varepsilon_d = -0.32$ eV) than the Y site ($\varepsilon_d = 0.23$ eV), indicating stronger adsorption at the Y site if following the d-band center theory. On the contrary, the larger Fermi softness of the Pt site ($S_f = 0.92$ eV⁻¹) compared with the Y site ($S_f = 0.30$ eV⁻¹) indicates the stronger adsorption atop the Pt site if following the Fermi softness theory. Hence, the Fermi softness theory can well describe the H adsorption at Pt₃Y, while the d-band center theory fails. The DOTA-PBE model can also accurately predict this case, with the predicted adsorption energies atop the Pt and Y sites being -2.75 eV and -0.88 eV, respectively. This surface is not included in our pretraining PBE dataset as well. The contribution of each energy level to the H adsorption was further elucidated by the integrated gradients algorithm. [87] It could be found from **Fig. 3c** that the Pt valence bands near the Fermi level account for the H chemisorption atop the Pt site, well aligning with the model of Fermi softness. Y conduct bands play a main role in the H chemisorption atop the Y site, which is consistent with the consensus that the strong Lewis acidity of Y could accept the electron of hydrogen. It indicates that the charge transfer induces the Y-H bonding, which explains the reason why the d-band center model is not suitable for describing this system. Hence, the DOTA-PBE model exhibits better generalization for the prediction of adsorption energies across metallic and intermetallic surfaces compared with traditional d-band center theory and Fermi softness theory.

Chemically accurate CO adsorption energy

Building upon the robust performance and transferability of DOTA-PBE, we further fine-tuned the model to achieve chemically accurate predictions of adsorption energies for specific adsorbates across metallic and intermetallic surfaces. The notable scarcity of chemically accurate adsorption energy data requires a model architecture with a minimum requirement of labeled chemically accurate adsorption energy data to fine-tune the model. Taking CO adsorption as an example, we first incorporated 988 LDOS-CO adsorption energy pairs (Table S2) across different sites of 174 metallic and intermetallic surfaces, evaluated by PBE, RPBE [88], and PBEsol [89] functionals, respectively. Data derived from different functionals expanded the perceptive chemical space, thereby enhancing the ability of the model to learn orbital interaction patterns between CO and metallic surfaces. Importantly, the foundation of PBE-level orbital interaction understanding, combined with GGA-level insights into CO-surface interactions, enabled exceptional data efficiency to achieve chemical accuracy predictions with only four high-fidelity data points. Each high-fidelity data point comprised experimentally measured CO adsorption energies (Pd(111), Cu(111), Ir(111), or Ni(111)) through precise microcalorimetry, paired with corresponding PBE-calculated surface LDOS profiles and HSE06-calculated gaseous CO LDOS characteristics (**Fig. 4a**). We compared adsorption energies of CO over Pt(111) and Rh(111) (**Fig. 4c**) predicted by the DOTA model with different input functional combinations for surface and adsorbate LDOS profiles with standard PBE, PBEsol, HSE06, RPA, and experimental results. As introduced from Blyholder’s model, [90] CO adsorption is primarily formed through the σ -donation between CO HOMO (5σ occupied orbital) and the metal conduction bands and the $d-\pi$ backbonding between CO LUMO ($2\pi^*$ unoccupied orbital) and the metal valence bands. Accordingly, the correct CO adsorption energy and binding sites rely on the correct description of the electronic structures of CO and the metallic surfaces. As reported previously, [91] HSE06 functional is poor at predicting CO adsorption because it fails to describe the delocalized electronic structures of metallic surfaces, while the underestimated HOMO-LUMO gap of CO by PBE and PBEsol functionals [92, 93] should account for the overbinding of CO over Pt(111) and Rh(111) surfaces. [94, 95] Moreover, these deficiencies result in the mistakenly predicted fcc sites for CO chemisorption over these two

surfaces. This manifests that the underestimated HOMO-LUMO gap by PBE functional is mainly responsible for the "CO puzzle", which was speculated by previous reports. Interestingly, despite the accurate CO adsorption energy, neither the CO HOMO-LUMO gap nor the metal cohesive energies could be accurately calculated by RPA (**Fig. 4**), which is consistent with previously reported results. [58] Importantly, HSE06 exhibits the best predictive performance for CO HOMO-LUMO energy levels, while PBE functional excels at the prediction of metal cohesive energy, indicating that HSE06 and PBE functionals are good at the description of the molecular orbitals and metal surfaces, respectively. Consequently, the input of HSE06-calculated gaseous CO LDOS characteristics and PBE-calculated surface LDOS profiles (HSE06/PBE) could provide superior results, with the predicted adsorption energy differing by less than 0.1 eV from the experimental values. More importantly, the model with the HSE06/PBE input combination could correctly predict the top site as the preferential binding site for CO adsorption, aligning with the experimental results. [18] The accuracy of the multimodal integration capitalizes on the advantages of the experimental precision of microcalorimetry in adsorption energy, the reliability of PBE functional for the description of electronic structures of metallic surfaces [96], and the superior performance of HSE06 beyond RPA for CO molecular orbital description [97, 84].

Discussion

The DOTA model integrates LDOSs from both the surface and the molecule as input. Different from the d-band center and Fermi level theories, this approach enables accurate prediction of adsorption energies across diverse adsorbates (MAE = 0.066 eV, MAPE = 1.53%) without reliance on predefined theoretical assumptions. Leveraging a Transformer architecture and integrated gradients algorithm, DOTA provides interpretable insights into the contribution of individual energy levels to adsorption strength. Established upon two key physical insights of the origin of the adsorption strength from orbital interactions and the functional-independent DOS-adsorption relationship, DOTA demonstrates its exceptional transferability. This permits integration of experimental sources and DFT data from different functionals and calculation settings. It could further achieve chemical accuracy in predicting molecular adsorption energies across extensive metallic and intermetallic surfaces, primarily trained on GGA-level datasets augmented by few-shot high-fidelity experimental adsorption energy data. Thus, DOTA represents a transformative leap forward in computational catalysis by addressing longstanding challenges such as functional dependency, limited availability of high-fidelity data, and the need for interpretable machine learning models. By synergizing deep learning architectures and physically informed features like LDOS, it achieves unprecedented accuracy and generalizability across chemical environments. Its capacity to unify multi-fidelity data sources and deliver mechanistic insights through interpretable attention paradigms establishes DOTA as a versatile framework for bridging experimental precision with computational efficiency. This could facilitate the construction of a large dataset of the adsorption energies with high fidelity, accelerating the discovery of next-generation catalysts and electrode materials.

Methods

All DFT calculations were performed with Vienna ab initio Simulation Package (VASP) [98, 99] with periodic boundary and the projector augmented wave (PAW) pseudopotentials [98, 100]. The Catalysis Kit (CatKit) software [44] and Atomic Simulation Environment (ASE) Python library [101, 102] were used for generating and classifying the adsorption structures. The chemisorption structures, except for CO adsorption, were obtained in reference [45] for DOTA model pretraining, where PBE functionals were used for both adsorption energy and DOS profile calculations. For CO adsorption, RPBE functional and PBEsol functional were also used for adsorption energy and DOS profile calculations, while the hybrid HSE06 functional was used only for electronic structure calculations. All calculations were conducted with spin polarization, using a kinetic energy cutoff of 450 eV. The $p(2 \times 2)$ 3-layer slab was employed for each metallic and intermetallic surface. The corresponding Monkhorst-Pack k-point grid [103] was $7 \times 7 \times 1$, with a first-order Methfessel-Paxton smearing of 0.1 eV. The resolution of calculated lm- and site-DOSs with reference to the Fermi level, which were employed for DOTA training, was 0.01 eV.

The DOTA model was implemented with the PyTorch Python library [104]. The AdamW optimizer with an initial learning rate of 0.0002 and the L_1 loss were used for training. An exponential cosine annealing scheduler was implemented to adjust the learning rate, and 150 epochs were used, with 50 epochs for warming up, and a batch size of 256. The contribution of each energy level to the adsorption energy was calculated using the interpretable integrated gradients algorithm implemented in the Captum library [87] with default parameters.

Code availability

Code for DOTA is available as an open source repository on GitHub, <https://github.com/zhzhang321/DOTA>

Competing interests

The authors declare no competing interests.

Acknowledgements

This work was supported by the National Key Research and Development Program of China (2023YFA1507601 and 2021YFA1500700). We thank the Center for High Performance Computing at Shanghai Jiao Tong University for providing the computing resources of the Siyuan-1 cluster.

Author contributions

Z.Zhang wrote the code and performed theoretical simulations. X.-M.C. designed the study, analyzed the data, and wrote the paper.

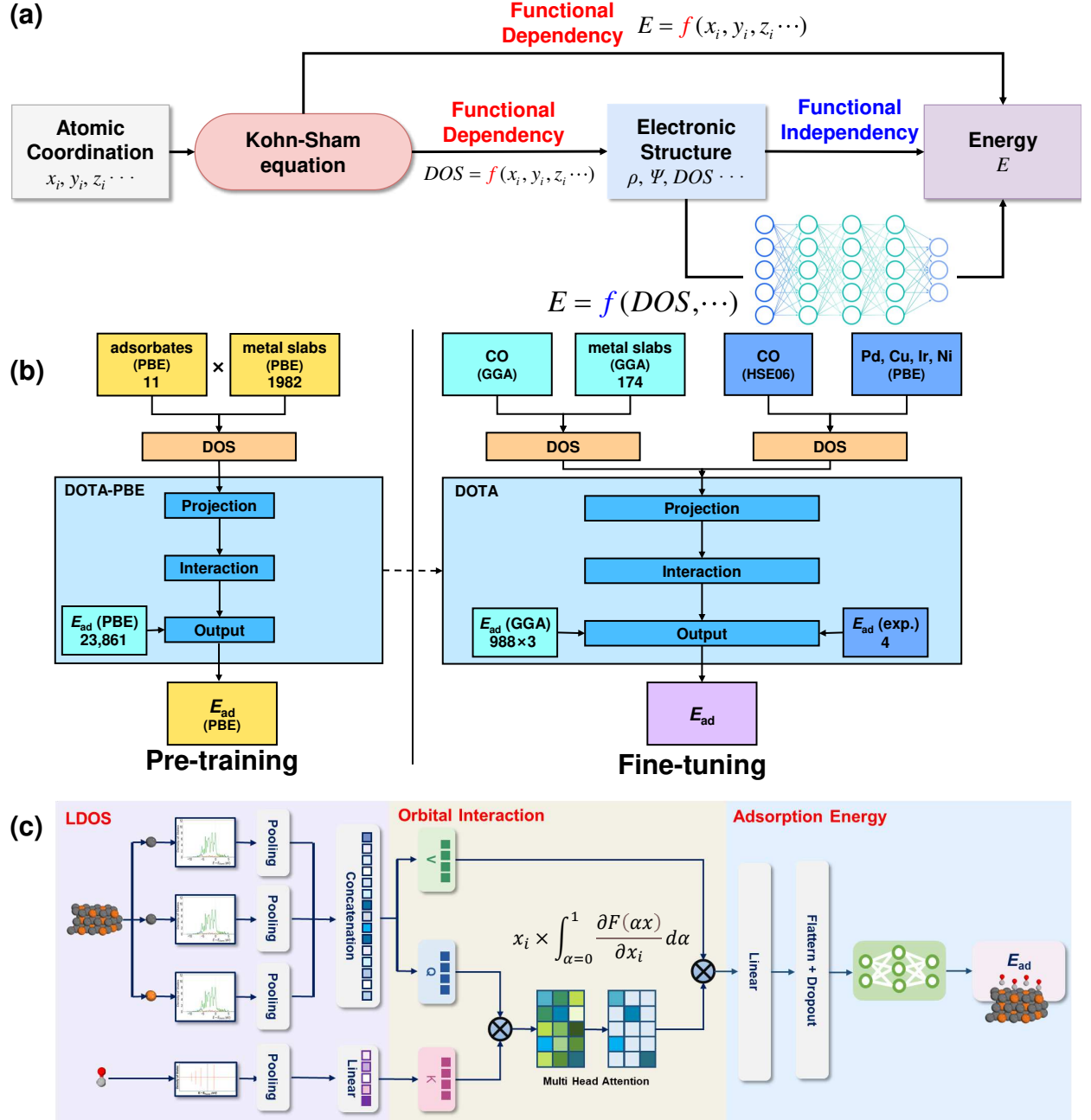


Figure 1: a) Procedure from coordination to energy. b) Pretraining and fine-tuning workflow of DOTA. c) Illustration of DOTA, with PDOS partition in lavender, orbital interaction in yellow, and output of adsorption energy in blue.

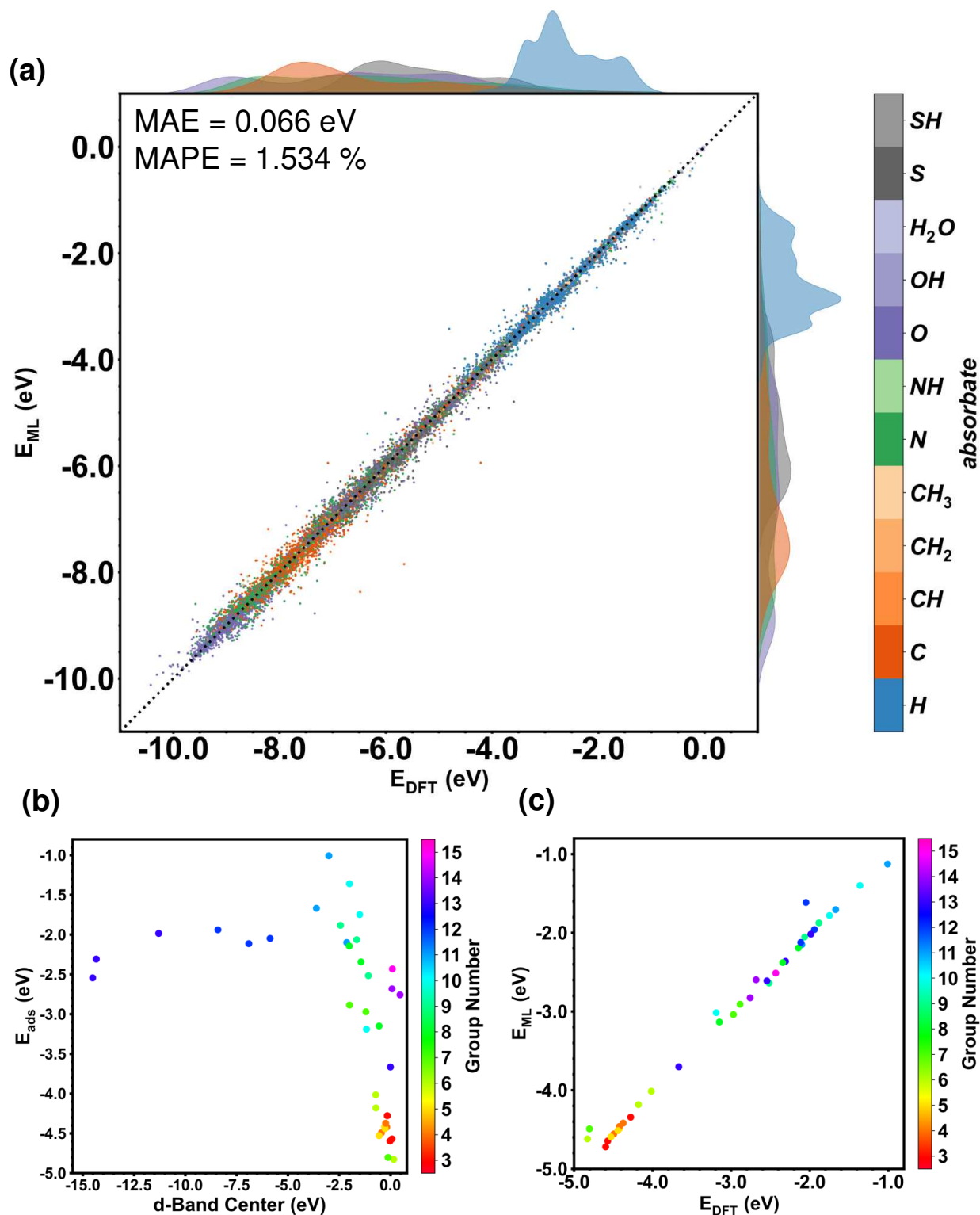


Figure 2: a) Parity plot and kernel density plot of adsorption energies between DFT calculated and DOTA predicted from five-fold cross-validation. b) Plot of d-band center versus DFT hydroxyl adsorption energy. c) Plot of DFT hydroxyl adsorption energy versus DOTA predicted energy.

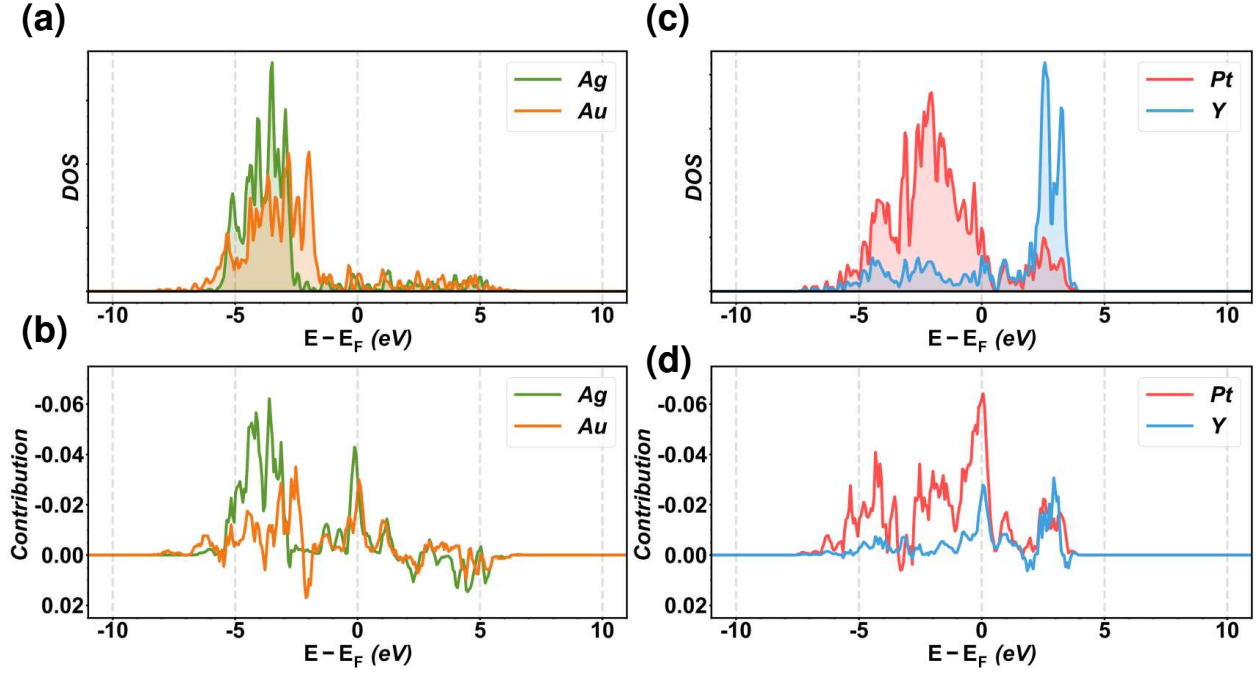


Figure 3: a) Density of states of surface Ag(Au) of Ag/Au(111) slab. b) Integrated gradients of Ag (Au) for OH adsorption on Ag/Au(111) top site. c) Density of states of platinum and Yttrium of Pt_3Y slab. d) Integrated gradients of platinum and yttrium for H adsorption on Pt_3Y the top site.

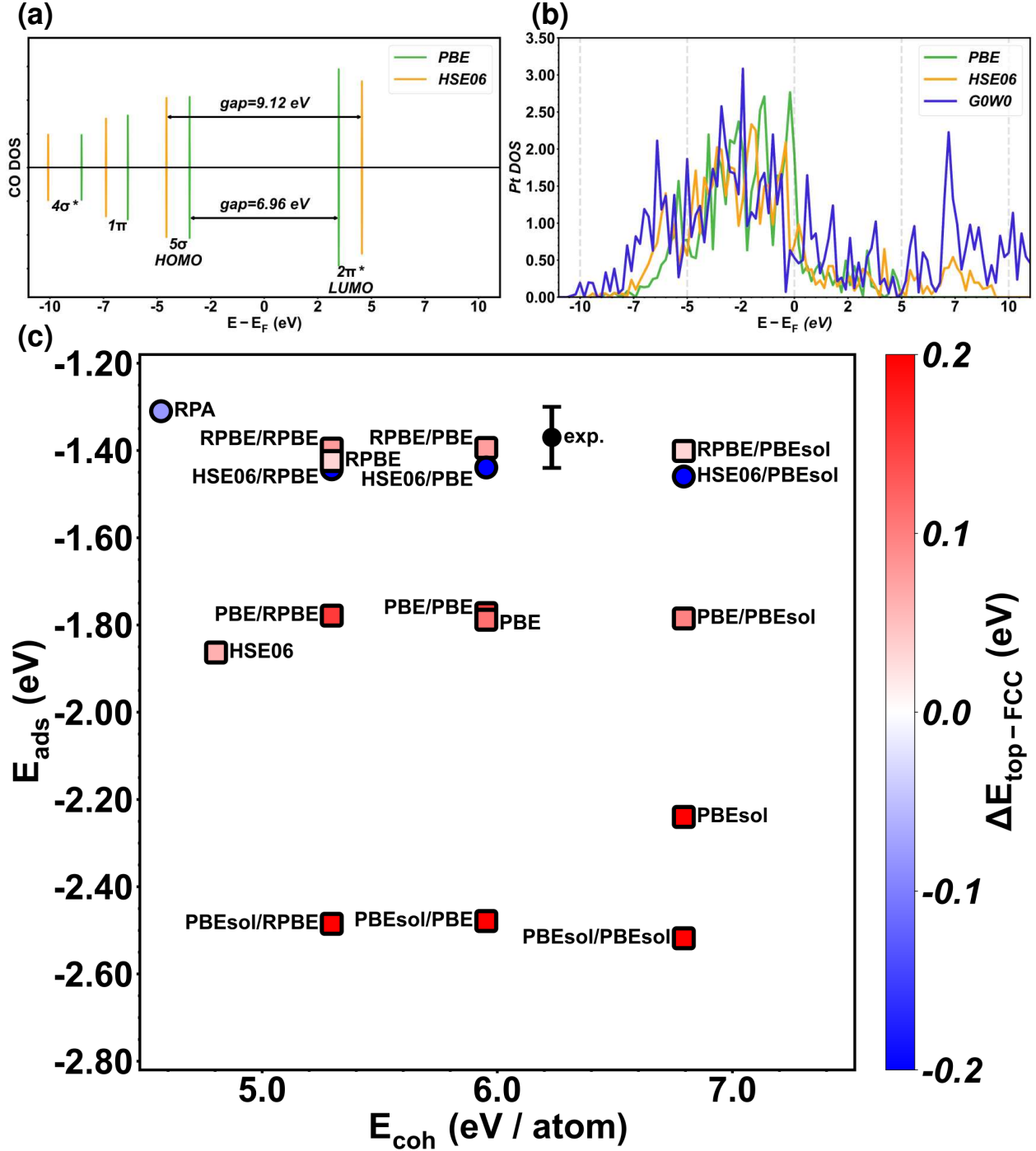


Figure 4: a) Density of states of CO obtained from different methods. b) Density of states of Pt slab obtained from different methods. c) Cohesive energies and predicted adsorption energies of various combinations of functionals. Only the adsorption energies for the preferred site are marked, and the difference between top and fcc sites is marked with color from blue to red. All predictions are labeled as functionals for adsorbates followed by functionals for metal slabs. Furthermore, some DFT calculations were conducted, including GGA functionals (PBE, RPBE, PBEsol), hybrid functionals (HSE06) and RPA method, which are labeled with the functionals or methods. The experience result is also marked with the label 'exp.'. Top site adsorptions are marked with circles, while fcc sites are marked with squares.

References

- [1] Yongxing He, Lin Yin, Niannian Yuan, and Gaoke Zhang. Adsorption and activation, active site and reaction pathway of photocatalytic CO₂ reduction: A review. *Chem. Eng. J.*, 481:148754, February 2024.
- [2] Junming Zhang, Hong Bin Yang, Daojin Zhou, and Bin Liu. Adsorption Energy in Oxygen Electrocatalysis. *Chem. Rev.*, 122(23):17028–17072, December 2022.
- [3] Zhen-Feng Huang, Jiajia Song, Shuo Dou, Xiaogang Li, Jiong Wang, and Xin Wang. Strategies to Break the Scaling Relation toward Enhanced Oxygen Electrocatalysis. *Matter*, 1(6):1494–1518, December 2019.
- [4] Yuechao Yang, Danxia Xu, Baolong Zhang, Zhimin Xue, and Tiancheng Mu. Substrate molecule adsorption energy: An activity descriptor for electrochemical oxidation of 5-Hydroxymethylfurfural (HMF). *Chem. Eng. J.*, 433:133842, April 2022.
- [5] Alexander Bagger, Wen Ju, Ana Sofia Varela, Peter Strasser, and Jan Rossmeisl. Electrochemical CO₂ Reduction: A Classification Problem. *ChemPhysChem*, 18(22):3266–3273, November 2017.
- [6] Dong Young Chung, Pietro P. Lopes, Pedro Farinazzo Bergamo Dias Martins, Haiying He, Tomoya Kawaguchi, Peter Zapol, Hoydoo You, Dusan Tripkovic, Dusan Strmcnik, Yisi Zhu, Soenke Seifert, Sungsik Lee, Vojislav R. Stamenkovic, and Nenad M. Markovic. Dynamic stability of active sites in hydr(oxy)oxides for the oxygen evolution reaction. *Nat. Energy*, 5(3):222–230, March 2020.
- [7] Xinyan Liu, Jianping Xiao, Hongjie Peng, Xin Hong, Karen Chan, and Jens K. Nørskov. Understanding trends in electrochemical carbon dioxide reduction rates. *Nat. Commun.*, 8(1):15438, May 2017.
- [8] Wesley Luc, Charles Collins, Siwen Wang, Hongliang Xin, Kai He, Yijin Kang, and Feng Jiao. Ag–Sn Bimetallic Catalyst with a Core–Shell Structure for CO₂ Reduction. *J. Am. Chem. Soc.*, 139(5):1885–1893, February 2017.
- [9] C.E. Borroni-Bird, N. Al-Sarraf, S. Andersoon, and D.A. King. Single crystal adsorption microcalorimetry. *Chem. Phys. Lett.*, 183(6):516–520, September 1991.
- [10] J. T. Stuckless, Nathan A. Frei, and Charles T. Campbell. A novel single-crystal adsorption calorimeter and additions for determining metal adsorption and adhesion energies. *Rev. Sci. Instrum.*, 69(6):2427–2438, June 1998.
- [11] N. Al-Sarraf, J.T. Stuckless, C.E. Wartnaby, and D.A. King. Adsorption microcalorimetry and sticking probabilities on metal single crystal surfaces. *Surf. Sci.*, 283(1-3):427–437, March 1993.
- [12] Eric M. Karp, Trent L. Silbaugh, Matthew C. Crowe, and Charles T. Campbell. Energetics of Adsorbed Methanol and Methoxy on Pt(111) by Microcalorimetry. *J. Am. Chem. Soc.*, 134(50):20388–20395, December 2012.
- [13] Jan-Henrik Fischer-Wolfarth, Jason A. Farmer, J. Manuel Flores-Camacho, Alexander Genest, Ilya V. Yudanov, Notker Rösch, Charles T. Campbell, Swetlana Schauermann, and Hans-Joachim Freund. Particle-size dependent heats of adsorption of CO on supported Pd nanoparticles as measured with a single-crystal microcalorimeter. *Phys. Rev. B*, 81(24):241416, June 2010.
- [14] Holger Dropsch and Manfred Baerns. CO adsorption on supported Pd catalysts studied by adsorption microcalorimetry and temperature programmed desorption. *Appl. Catal. A: Gen.*, 158(1-2):163–183, September 1997.
- [15] Ole Lytken, Wanda Lew, Jonathan J. W. Harris, Ebbe K. Vestergaard, J. Michael Gottfried, and Charles T. Campbell. Energetics of Cyclohexene Adsorption and Reaction on Pt(111) by Low-Temperature Microcalorimetry. *J. Am. Chem. Soc.*, 130(31):10247–10257, August 2008.
- [16] Zhongtian Mao, John R. Rumpitz, and Charles T. Campbell. Energetics of Ag Adsorption on and Adhesion to Rutile TiO₂ (100) Studied by Microcalorimetry. *J. Phys. Chem. C*, 125(5):3036–3046, February 2021.
- [17] Luis E. Botello, Marco Schöning, José Solla-Gullón, Víctor Climent, Juan M. Feliu, and Rolf Schuster. Direct measurement of the hydrogen adsorption entropy on shape-controlled Pt nanoparticles using electrochemical microcalorimetry. *J. Mater. Chem. A*, 12(1):184–191, 2024.
- [18] Jess Wellendorff, Trent L. Silbaugh, Delfina Garcia-Pintos, Jens K. Nørskov, Thomas Bligaard, Felix Studt, and Charles T. Campbell. A benchmark database for adsorption bond energies to transition metal surfaces and comparison to selected DFT functionals. *Surf. Sci.*, 640:36–44, October 2015.
- [19] Reinhard J. Maurer, Victor G. Ruiz, Javier Camarillo-Cisneros, Wei Liu, Nicola Ferri, Karsten Reuter, and Alexandre Tkatchenko. Adsorption structures and energetics of molecules on metal surfaces: Bridging experiment and theory. *Prog. Surf. Sci.*, 91(2):72–100, May 2016.

- [20] Breanna M. Wong, Greg Collinge, Alyssa J.R. Hensley, Yong Wang, and Jean-Sabin McEwen. Benchmarking the accuracy of coverage-dependent models: Adsorption and desorption of benzene on Pt (1 1 1) and Pt₃Sn (1 1 1) from first principles. *Prog. Surf. Sci.*, 94(2):100538, May 2019.
- [21] Claudio Cazorla. The role of density functional theory methods in the prediction of nanostructured gas-adsorbent materials. *Coord. Chem. Rev.*, 300:142–163, September 2015.
- [22] Joachim Sauer. Ab Initio Calculations for Molecule–Surface Interactions with Chemical Accuracy. *Acc. Chem. Res.*, 52(12):3502–3510, December 2019.
- [23] Xinyan Liu and Hong-Jie Peng. Toward Next-Generation Heterogeneous Catalysts: Empowering Surface Reactivity Prediction with Machine Learning. *Engineering*, 39:25–44, August 2024.
- [24] Bin Wang and Fuxiang Zhang. Main Descriptors To Correlate Structures with the Performances of Electrocatalysts. *Angew. Chem. Int. Ed.*, 61(4):e202111026, January 2022.
- [25] Qiang Gao, Hemanth Somarajan Pillai, Yang Huang, Shikai Liu, Qingmin Mu, Xue Han, Zihao Yan, Hua Zhou, Qian He, Hongliang Xin, and Huiyuan Zhu. Breaking adsorption-energy scaling limitations of electrocatalytic nitrate reduction on intermetallic CuPd nanocubes by machine-learned insights. *Nat. Commun.*, 13(1):2338, April 2022.
- [26] Jack K. Pedersen, Thomas A. A. Batchelor, Alexander Bagger, and Jan Rossmeisl. High-Entropy Alloys as Catalysts for the CO₂ and CO Reduction Reactions. *ACS Catal.*, 10(3):2169–2176, February 2020.
- [27] Zhao Li, Benjamin J. Bucior, Haoyuan Chen, Maciej Haranczyk, J. Ilja Siepmann, and Randall Q. Snurr. Machine learning using host/guest energy histograms to predict adsorption in metal–organic frameworks: Application to short alkanes and Xe/Kr mixtures. *J. Chem. Phys.*, 155(1):014701, July 2021.
- [28] B. Moses Abraham, Oriol Piqué, Mohd Aamir Khan, Francesc Viñes, Francesc Illas, and Jayant K. Singh. Machine Learning-Driven Discovery of Key Descriptors for CO₂ Activation over Two-Dimensional Transition Metal Carbides and Nitrides. *ACS Appl. Mater. Interfaces*, 15(25):30117–30126, June 2023.
- [29] Osman Mamun, Kirsten T. Winther, Jacob R. Boes, and Thomas Bligaard. A Bayesian framework for adsorption energy prediction on bimetallic alloy catalysts. *npj Comput. Mater.*, 6(1):177, November 2020.
- [30] Zhuole Lu, Shwetank Yadav, and Chandra Veer Singh. Predicting aggregation energy for single atom bimetallic catalysts on clean and O* adsorbed surfaces through machine learning models. *Catal. Sci. Technol.*, 10(1):86–98, 2020.
- [31] Benjamin M. Comer, Neha Bothra, Jaclyn R. Lunger, Frank Abild-Pedersen, Michal Bajdich, and Kirsten T. Winther. Prediction of O and OH Adsorption on Transition Metal Oxide Surfaces from Bulk Descriptors. *ACS Catal.*, 14(7):5286–5296, April 2024.
- [32] Shreya Sinha, Bruno Mladineo, Ivor Lončarić, and Peter Saalfrank. Multidimensional Neural Network Interatomic Potentials for CO on NaCl(100). *J. Phys. Chem. C*, 128(49):21117–21131, December 2024.
- [33] Joseph H. Montoya and Kristin A. Persson. A high-throughput framework for determining adsorption energies on solid surfaces. *npj Comput. Mater.*, 3(1):14, March 2017.
- [34] Kamal Choudhary, Taner Yildirim, Daniel W. Siderius, A. Gilad Kusne, Austin McDannald, and Diana L. Ortiz-Montalvo. Graph neural network predictions of metal organic framework CO₂ adsorption properties. *Comput. Mater. Sci.*, 210:111388, July 2022.
- [35] Qi Wang and Yonggang Yao. Harnessing machine learning for high-entropy alloy catalysis: A focus on adsorption energy prediction. *npj Comput. Mater.*, 11(1):91, April 2025.
- [36] Sergio Pablo-García, Santiago Morandi, Rodrigo A. Vargas-Hernández, Kjell Jorner, Žarko Ivković, Núria López, and Alán Aspuru-Guzik. Fast evaluation of the adsorption energy of organic molecules on metals via graph neural networks. *Nat. Comput. Sci.*, 3(5):433–442, May 2023.
- [37] Joakim S. Jestilä, Nian Wu, Fabio Priante, and Adam S. Foster. Accelerated Lignocellulosic Molecule Adsorption Structure Determination. *J. Chem. Theory Comput.*, 20(5):2297–2312, March 2024.
- [38] Steffen Jeschke, Karen Wilson, and Adam F. Lee. Accelerating Computational Modeling of Reactant Adsorption through a Combined MACE+DFT Approach: Furfural on Cu Surfaces. *J. Phys. Chem. C*, 129(26):11948–11957, July 2025.
- [39] Kameswari Gnana Asritha Varanasi and Kaihang Shi. *Understanding the Behavior of Machine Learning Potentials for Simulation of Gas Adsorption*. PhD thesis, State University of New York at Buffalo, United States – New York, 2025.

- [40] Olga Klimanova, Nikita Rybin, and Alexander Shapeev. Accelerating the global search of adsorbate molecule positions using machine-learning interatomic potentials with active learning. *Phys. Chem. Chem. Phys.*, 27(17):9201–9210, 2025.
- [41] Janice Lan, Aini Palizhati, Muhammed Shuaibi, Brandon M. Wood, Brook Wander, Abhishek Das, Matt Uyttendaele, C. Lawrence Zitnick, and Zachary W. Ulissi. AdsorbML: A leap in efficiency for adsorption energy calculations using generalizable machine learning potentials. *npj Comput. Mater.*, 9(1):172, September 2023.
- [42] Lowik Chanussot, Abhishek Das, Siddharth Goyal, Thibaut Lavril, Muhammed Shuaibi, Morgane Riviere, Kevin Tran, Javier Heras-Domingo, Caleb Ho, Weihua Hu, Aini Palizhati, Anuroop Sriram, Brandon Wood, Junwoong Yoon, Devi Parikh, C. Lawrence Zitnick, and Zachary Ulissi. Open catalyst 2020 (OC20) dataset and community challenges. *ACS Catal.*, 11(10):6059–6072, May 2021.
- [43] Richard Tran, Janice Lan, Muhammed Shuaibi, Brandon M. Wood, Siddharth Goyal, Abhishek Das, Javier Heras-Domingo, Adeesh Kolluru, Ammar Rizvi, Nima Shoghi, Anuroop Sriram, Félix Therrien, Jehad Abed, Oleksandr Voznyy, Edward H. Sargent, Zachary Ulissi, and C. Lawrence Zitnick. The open catalyst 2022 (OC22) dataset and challenges for oxide electrocatalysts. *ACS Catal.*, 13(5):3066–3084, 2023.
- [44] Kirsten T. Winther, Max J. Hoffmann, Jacob R. Boes, Osman Mamun, Michal Bajdich, and Thomas Bligaard. Catalysis-hub.org, an open electronic structure database for surface reactions. *Sci. Data*, 6(1):75, May 2019.
- [45] Osman Mamun, Kirsten T. Winther, Jacob R. Boes, and Thomas Bligaard. High-throughput calculations of catalytic properties of bimetallic alloy surfaces. *Sci. Data*, 6(1):76, May 2019.
- [46] Xu Huang, Bowen Deng, Peichen Zhong, Aaron D. Kaplan, Kristin A. Persson, and Gerbrand Ceder. Cross-functional transferability in universal machine learning interatomic potentials, 2025.
- [47] Chi Chen, Yunxing Zuo, Weiye Ye, Xiangguo Li, and Shyue Ping Ong. Learning properties of ordered and disordered materials from multi-fidelity data. *Nat. Comput. Sci.*, 1(1):46–53, January 2021.
- [48] Tsz Wai Ko and Shyue Ping Ong. Data-efficient construction of high-fidelity graph deep learning interatomic potentials. *npj Comput. Mater.*, 11(1):65, March 2025.
- [49] Alice E. A. Allen, Nicholas Lubbers, Sakib Matin, Justin Smith, Richard Messerly, Sergei Tretiak, and Kipton Barros. Learning together: Towards foundation models for machine learning interatomic potentials with meta-learning. *npj Comput. Mater.*, 10(1):154, July 2024.
- [50] Jaesun Kim, Jisu Kim, Jaehoon Kim, Jiho Lee, Yutack Park, Youngho Kang, and Seungwu Han. Data-efficient multifidelity training for high-fidelity machine learning interatomic potentials. *J. Am. Chem. Soc.*, 147(1):1042–1054, January 2025.
- [51] John P. Perdew, Kieron Burke, and Matthias Ernzerhof. Generalized gradient approximation made simple. *Phys. Rev. Lett.*, 77(18):3865–3868, October 1996.
- [52] Jess Wellendorff, Keld T. Lundgaard, Andreas Møgelhøj, Vivien Petzold, David D. Landis, Jens K. Nørskov, Thomas Bligaard, and Karsten W. Jacobsen. Density functionals for surface science: Exchange-correlation model development with bayesian error estimation. *Phys. Rev. B*, 85(23):235149, June 2012.
- [53] Anubhav Jain, Shyue Ping Ong, Geoffroy Hautier, Wei Chen, William Davidson Richards, Stephen Dacek, Shreyas Cholia, Dan Gunter, David Skinner, Gerbrand Ceder, and Kristin A. Persson. Commentary: The materials project: A materials genome approach to accelerating materials innovation. *APL Mater.*, 1(1):011002, July 2013.
- [54] Peter J. Feibelman, B. Hammer, J. K. Nørskov, F. Wagner, M. Scheffler, R. Stumpf, R. Watwe, and J. Dumesic. The CO/pt(111) puzzle. *J. Phys. Chem. B*, 105(18):4018–4025, May 2001.
- [55] Ilya Grinberg, Yashar Yourdshahyan, and Andrew M. Rappe. CO on pt(111) puzzle: A possible solution. *J. Chem. Phys.*, 117(5):2264–2270, August 2002.
- [56] Marek Gajdoš, Andreas Eichler, and Jürgen Hafner. CO adsorption on close-packed transition and noble metal surfaces: Trends from ab initio calculations. *J. Phys.: Condens. Matter*, 16(8):1141, February 2004.
- [57] Alessandro Stroppa, Konstantinos Termentzidis, Joachim Paier, Georg Kresse, and Jürgen Hafner. CO adsorption on metal surfaces: A hybrid functional study with plane-wave basis set. *Phys. Rev. B*, 76(19):195440, November 2007.
- [58] L. Schimka, J. Harl, A. Stroppa, A. Grüneis, M. Marsman, F. Mittendorfer, and G. Kresse. Accurate surface and adsorption energies from many-body perturbation theory. *Nat. Mater.*, 9(9):741–744, September 2010.
- [59] Jianwei Sun, Adrienn Ruzsinszky, and John P. Perdew. Strongly constrained and appropriately normed semilocal density functional. *Phys. Rev. Lett.*, 115(3):036402, July 2015.

- [60] James W. Furness, Aaron D. Kaplan, Jinliang Ning, John P. Perdew, and Jianwei Sun. Accurate and numerically efficient r2SCAN meta-generalized gradient approximation. *J. Phys. Chem. Lett.*, 11(19):8208–8215, October 2020.
- [61] Abhirup Patra, Haowei Peng, Jianwei Sun, and John P. Perdew. Rethinking CO adsorption on transition-metal surfaces: Effect of density-driven self-interaction errors. *Phys. Rev. B*, 100(3):035442, July 2019.
- [62] Lars Hedin. New method for calculating the one-particle green’s function with application to the electron-gas problem. *Phys. Rev.*, 139(3A):A796–A823, August 1965.
- [63] Adam Kubas, Daniel Berger, Harald Oberhofer, Dimitrios Maganas, Karsten Reuter, and Frank Neese. Surface adsorption energetics studied with “gold standard” wave-function-based ab initio methods: Small-molecule binding to TiO₂(110). *J. Phys. Chem. Lett.*, 7(20):4207–4212, October 2016.
- [64] Carsten Müller, Björn Herschend, Kersti Hermansson, and Beate Paulus. Application of the method of increments to the adsorption of CO on the CeO₂(110) surface. *J. Chem. Phys.*, 128(21):214701, June 2008.
- [65] Christopher Sheldon, Joachim Paier, Denis Usvyat, and Joachim Sauer. Hybrid RPA:DFT approach for adsorption on transition metal surfaces: Methane and ethane on platinum (111). *J. Chem. Theory Comput.*, 20(5):2219–2227, March 2024.
- [66] Xinguo Ren, Patrick Rinke, and Matthias Scheffler. Exploring the random phase approximation: Application to CO adsorbed on cu(111). *Phys. Rev. B*, 80(4):045402, July 2009.
- [67] Peitao Liu, Jiantao Wang, Noah Avargues, Carla Verdi, Andreas Singraber, Ferenc Karsai, Xing-Qiu Chen, and Georg Kresse. Combining machine learning and many-body calculations: Coverage-dependent adsorption of CO on rh(111). *Phys. Rev. Lett.*, 130(7):078001, February 2023.
- [68] Raghunathan Ramakrishnan, Pavlo O. Dral, Matthias Rupp, and O. Anatole von Lilienfeld. Big data meets quantum chemistry approximations: The Δ -machine learning approach. *J. Chem. Theory Comput.*, 11(5):2087–2096, May 2015.
- [69] Albert P. Bartók, Sandip De, Carl Poelking, Noam Bernstein, James R. Kermode, Gábor Csányi, and Michele Ceriotti. Machine learning unifies the modeling of materials and molecules. *Sci. Adv.*, 3(12):e1701816, December 2017.
- [70] Albert P. Bartók, Michael J. Gillan, Frederick R. Manby, and Gábor Csányi. Machine-learning approach for one- and two-body corrections to density functional theory: Applications to molecular and condensed water. *Phys. Rev. B*, 88(5):054104, August 2013.
- [71] B. Hammer and J.K. Nørskov. Electronic factors determining the reactivity of metal surfaces. *Surf. Sci.*, 343(3):211–220, 1995.
- [72] A. Vojvodic, J. K. Nørskov, and F. Abild-Pedersen. Electronic structure effects in transition metal surface chemistry. *Top. Catal.*, 57(1):25–32, February 2014.
- [73] P. W. Anderson. Localized magnetic states in metals. *Phys. Rev.*, 124(1):41–53, October 1961.
- [74] D.M. Edwards and D.M. Newns. Electron interaction in the band theory of chemisorption. *Phys. Lett. A*, 24(4):236–237, 1967.
- [75] T B Grimley. The indirect interaction between atoms or molecules adsorbed on metals. *Proc. Phys. Soc.*, 90(3):751, March 1967.
- [76] Siwen Wang, Hemanth Somarajan Pillai, and Hongliang Xin. Bayesian learning of chemisorption for bridging the complexity of electronic descriptors. *Nat. Commun.*, 11(1):6132, November 2020.
- [77] Bing Huang, Li Xiao, Juntao Lu, and Lin Zhuang. Spatially resolved quantification of the surface reactivity of solid catalysts. *Angew. Chem. Int. Ed.*, 55(21):6239–6243, 2016.
- [78] Victor Fung, Guoxiang Hu, P. Ganesh, and Bobby G. Sumpter. Machine learned features from density of states for accurate adsorption energy prediction. *Nat. Commun.*, 12(1):88, January 2021.
- [79] Lynn Vonder Haar, Timothy Elvira, and Omar Ochoa. An analysis of explainability methods for convolutional neural networks. *Eng. Appl. Artif. Intell.*, 117:105606, 2023.
- [80] Nadia Burkart and Marco F. Huber. A survey on the explainability of supervised machine learning. *J. Artif. Intell. Res.*, 70:245–317, January 2021.
- [81] Chester V. Dolph, Loc Tran, and Bonnie D. Allen. Towards explainability of UAV-based convolutional neural networks for object classification. In *2018 Aviat. Technol. Integr. Oper. Conf.*, Atlanta, GA, June 2018.
- [82] Feiniu Yuan, Zhengxiao Zhang, and Zhijun Fang. An effective CNN and transformer complementary network for medical image segmentation. *Pattern Recognit.*, 136:109228, 2023.

- [83] Honglin Wu, Peng Huang, Min Zhang, Wenlong Tang, and Xinyu Yu. CMTFNet: CNN and multiscale transformer fusion network for remote-sensing image semantic segmentation. *IEEE Trans. Geosci. Remote Sens.*, 61:1–12, 2023.
- [84] Aliaksandr V. Kravau, Oleg A. Vydrov, Artur F. Izmaylov, and Gustavo E. Scuseria. Influence of the exchange screening parameter on the performance of screened hybrid functionals. *J. Chem. Phys.*, 125(22):224106, December 2006.
- [85] Matthew M. Montemore and J. Will Medlin. A simple, accurate model for alkyl adsorption on late transition metals. *The Journal of Physical Chemistry C*, 117(6):2835–2843, February 2013.
- [86] Hongliang Xin and Suljo Linic. Communications: Exceptions to the d-band model of chemisorption on metal surfaces: The dominant role of repulsion between adsorbate states and metal d-states. *The Journal of Chemical Physics*, 132(22):221101, June 2010.
- [87] Narine Kokhlikyan, Vivek Miglani, Miguel Martin, Edward Wang, Bilal Alsallakh, Jonathan Reynolds, Alexander Melnikov, Natalia Kliushkina, Carlos Araya, Siqi Yan, and Orion Reblitz-Richardson. Captum: A unified and generic model interpretability library for PyTorch, 2020.
- [88] B. Hammer, L. B. Hansen, and J. K. Nørskov. Improved adsorption energetics within density-functional theory using revised perdue-burke-ernzerhof functionals. *Phys. Rev. B*, 59(11):7413–7421, March 1999.
- [89] John P. Perdew, Adrienn Ruzsinszky, Gábor I. Csonka, Oleg A. Vydrov, Gustavo E. Scuseria, Lucian A. Constantin, Xiaolan Zhou, and Kieron Burke. Restoring the density-gradient expansion for exchange in solids and surfaces. *Phys. Rev. Lett.*, 100(13):136406, April 2008.
- [90] George Blyholder. Molecular orbital view of chemisorbed carbon monoxide. *The Journal of Physical Chemistry*, 68(10):2772–2777, October 1964.
- [91] A Stroppa and G Kresse. The shortcomings of semi-local and hybrid functionals: What we can learn from surface science studies. *New J. Phys.*, 10(6):063020, June 2008.
- [92] Neil Qiang Su and Xin Xu. Insights into direct methods for predictions of ionization potential and electron affinity in density functional theory. *The Journal of Physical Chemistry Letters*, 10(11):2692–2699, June 2019.
- [93] Neil Qiang Su and Xin Xu. Perturbation theory made efficient and effective for predictions of ionization potential and electron affinity. *The Journal of Chemical Physics*, 154(17):174101, May 2021.
- [94] Sahar Sharifzadeh, Patrick Huang, and Emily Carter. Embedded configuration interaction description of CO on cu(111): Resolution of the site preference conundrum. *J. Phys. Chem. C*, 112(12):4649–4657, March 2008.
- [95] Alfred Gil, Anna Clotet, Josep M. Ricart, Georg Kresse, Maite García-Hernández, Notker Rösch, and Philippe Sautet. Site preference of CO chemisorbed on pt(111) from density functional calculations. *Surf. Sci.*, 530(1):71–87, 2003.
- [96] M. Ropo, K. Kokko, and L. Vitos. Assessing the perdue-burke-ernzerhof exchange-correlation density functional revised for metallic bulk and surface systems. *Phys. Rev. B*, 77(19):195445, May 2008.
- [97] Alejandro J. Garza and Gustavo E. Scuseria. Predicting band gaps with hybrid density functionals. *J. Phys. Chem. Lett.*, 7(20):4165–4170, October 2016.
- [98] G. Kresse and J. Furthmüller. Efficiency of ab-initio total energy calculations for metals and semiconductors using a plane-wave basis set. *Comput. Mater. Sci.*, 6(1):15–50, 1996.
- [99] G. Kresse and J. Furthmüller. Efficient iterative schemes for ab initio total-energy calculations using a plane-wave basis set. *Phys. Rev. B*, 54(16):11169–11186, October 1996.
- [100] P. E. Blöchl. Projector augmented-wave method. *Phys. Rev. B*, 50(24):17953–17979, December 1994.
- [101] S. R. Bahn and K. W. Jacobsen. An object-oriented scripting interface to a legacy electronic structure code. *Comput. Sci. Eng.*, 4(3):56–66, May 2002.
- [102] Ask Hjorth Larsen, Jens Jørgen Mortensen, Jakob Blomqvist, Ivano E Castelli, Rune Christensen, Marcin Dułak, Jesper Friis, Michael N Groves, Bjørk Hammer, Cory Hargus, Eric D Hermes, Paul C Jennings, Peter Bjerre Jensen, James Kermode, John R Kitchin, Esben Leonhard Kolsbjerg, Joseph Kubal, Kristen Kaasbjerg, Steen Lysgaard, Jón Bergmann Maronsson, Tristan Maxson, Thomas Olsen, Lars Pastewka, Andrew Peterson, Carsten Rostgaard, Jakob Schiøtz, Ole Schütt, Mikkel Strange, Kristian S Thygesen, Tejs Vegge, Lasse Vilhelmsen, Michael Walter, Zhenhua Zeng, and Karsten W Jacobsen. The atomic simulation environment—a python library for working with atoms. *J. Phys. Condens. Matter*, 29(27):273002, June 2017.
- [103] Hendrik J. Monkhorst and James D. Pack. Special points for brillouin-zone integrations. *Phys. Rev. B*, 13(12):5188–5192, June 1976.

- [104] Adam Paszke, Sam Gross, Francisco Massa, Adam Lerer, James Bradbury, Gregory Chanan, Trevor Killeen, Zeming Lin, Natalia Gimelshein, Luca Antiga, Alban Desmaison, Andreas Kopf, Edward Yang, Zachary DeVito, Martin Raison, Alykhan Tejani, Sasank Chilamkurthy, Benoit Steiner, Lu Fang, Junjie Bai, and Soumith Chintala. PyTorch: An imperative style, high-performance deep learning library. In *Advances in Neural Information Processing Systems 32*, pages 8024–8035. Curran Associates, Inc., 2019.

PREDICTING CHEMICALLY ACCURATE ADSORPTION ENERGY USING AN INTERPRETABLE DEEP LEARNING MODEL PRETRAINED BY GGA CALCULATION DATA

Zhihao Zhang¹ and Xiao-Ming Cao^{1,2,*}

¹State Key Laboratory of Green Chemical Engineering and Industrial Catalysis, Centre for Computational Chemistry and Research Institute of Industrial Catalysis, East China University of Science and Technology, Shanghai 200237, China

²State Key Laboratory of Synergistic Chem-Bio Synthesis, School of Chemistry and Chemical Engineering, Shanghai Jiao Tong University, Shanghai 200240, China

*Corresponding author: xmcao@sjtu.edu.cn

July 29, 2025

Table S1: Performance of DOTA for different adsorbates

Adsorbate	Counts	Average (eV)	SD (eV)	MAE (eV)	MAPE (%)	RMSE (eV)
H	5453	-2.579	0.707	0.042	1.747	0.075
C	4197	-6.376	1.715	0.083	1.322	0.135
CH	107	-5.232	1.710	0.082	1.522	0.133
CH ₂	82	-3.808	1.340	0.060	1.654	0.089
CH ₃	75	-1.933	0.761	0.044	3.440	0.063
N	4418	-6.058	1.971	0.074	1.340	0.115
NH	104	-5.238	1.948	0.096	1.775	0.135
O	4940	-6.293	1.871	0.071	1.190	0.115
OH	98	-3.810	1.344	0.079	2.307	0.111
H ₂ O	60	-0.417	0.368	0.061	49.632	0.114
S	4227	-5.195	1.212	0.066	1.307	0.106
SH	100	-2.427	1.097	0.053	2.664	0.078
Total	23861	-5.148	2.172	0.066	1.534	0.109

Table S2: Data used for training DOTA

Adsorbate	Counts	Functional for DOS	Functional for Energy	Surfaces
H	5453	PBE	PBE	metallic and bimetallic alloy (111) surfaces with the combination of 37 metals (Sc, Ti, V, Cr, Mn, Fe, Co, Ni, Cu, Zn, Y, Zr, Nb, Mo, Tc, Ru, Rh, Pd, Ag, Cd, La, Hf, Ta, W, Re, Os, Ir, Pt, Au, Hg, Al, Ga, In, Sn, Tl, Pb, Bi)
C	4197			
CH	107			
CH₂	82			
CH₃	75			
N	4418			
NH	104			
O	4940			
OH	98			
H₂O	60			
S	4227			
SH	100			
CO	988	PBE	PBE	metallic and bimetallic alloy (111) surfaces with the combination of 11 metals (Co, Ni, Cu, Rh, Pd, Ag, Ir, Pt, Au, Sn, Pb)
CO	988	RPBE	RPBE	
CO	988	PBESol	PBESol	
CO	4	PBE (slab) + HSE06 (adsorbate)	Exp.	Pd(111)(fcc), Cu(111)(top), Ir(111) (fcc), Ni(111)(fcc)